# Uptake of Hydrogen Halides by Water Droplets

**Francis Schweitzer, Philippe Mirabel, and Christian George*,†**

*Centre de Géochimie de la Surface/Centre National de la Recherche Scientifique and Université Louis Pasteur, 28 rue Goethe, F-67083 Strasbourg, France*

*Received: July 27, 1999; In Final Form: October 20, 1999*

The uptake kinetics of three different hydrogen halides, i.e., HCl, HBr, and HI, by aqueous surfaces were measured as a function of temperature in the range from 262 to 281 K using the droplet train technique. The reported mass accommodation coefficients ($\alpha$) were shown to decrease with increasing temperature. For HCl, $\alpha$ decreases from 0.24 to 0.13 when the temperature was raised from 263 to 281 K. In the same temperature range, the mass accommodation of HBr and HI decrease from 0.16 to 0.068 and 0.19 to 0.079, respectively. This temperature trend suggests that the rate-limiting step during the accommodation process is part of the physical solvation process as previously reported for nonreacting gases. The data were accordingly interpreted using a model found in the literature which describes the mass accommodation process as a dynamical nucleation event. The implications for the tropospheric chemistry of these findings are also discussed.

## Introduction

It has been shown over the years that heterogeneous or multiphase chemical transformations within the atmosphere may strongly alter its oxidation capacity especially by keeping in their reactive form given families of radicals.[1] In fact, the observation since the mid 1970s of the stratospheric ozone hole and more recently the discovery of so-called "halogen explosion" in the Arctic's boundary layer[2] underlined the importance of chemical conversions at the gas/liquid interface.

In the marine boundary layer, the origin of halogenated radicals in the gas phase has been attributed to transformations occurring on sea-salt aerosols.[3] Several hints supported this hypothesis. In fact, it has been shown for a long time that sea-salt aerosols may display a large deficit in chloride compared to the original composition of seawater. Since the mechanisms producing these aerosols (i.e., wave breaking and bubble ejection) should not affect their composition, the observed deficit was generally attributed to the displacement of halogenated inorganic acids due to the uptake, by the aerosols, of strong acids ($HNO_3$ or $H_2SO_4$).[4] In some cases, the observed deficit reached even 90% of the original chloride content; however, as noted by Keene et al.,[5] such a deficit cannot be explained by acid displacement alone. Accordingly many authors postulated that other reactions are involved in which stable ions are transformed into halogenated radical precursors. The chemical mechanism leading to the formation of the observed levels of Cl radicals is still under discussion but it is now clear that it depends on the environment where the halogen activation take place, i.e., in $NO_x$-free (in the Arctic for example) or polluted coastal regions. For the latter, it has been shown that the chemistry of dinitrogen pentoxide is very important since it produces large amount of easily photolyzable substances i.e., nitryl compounds (see refs 3 and 6−9 for a thorough discussion of that chemical system). Whereas, in a $NO_x$-free region, the halogen activation is thought to proceed, among other currently discussed reaction schemes, via aqueous phase photoproduction of $Br_2$ that will introduce reaction cycles involving hypohalogeneous acids that will give birth to the so-called "halogen explosion".[10−12]

In both cases, however, the levels of halogenated radicals are large enough to strongly modify the local or regional oxidation capacity. In fact, in a polluted zone, the measured Cl atom concentrations[5] are in the range $10^4-10^5$ cm$^{-3}$ which would imply, for example, a significant enhancement of the oxidation rates of nonmethane hydrocarbons (NMHC). Such an enhancement was indeed observed in Lagrangian type field experiments,[13] where it was shown that OH oxidation alone was unable to describe the measured NMHC decay. The latter being consistent with a Cl atom concentration of about $6 \times 10^4$ cm$^{-3}$ at noon.[13]

Most of the recent available data have been implemented in up-to-date box model in which chemistry is simulated with great details;[10,11] however, there is still a lack of knowledge concerning the rate of mass transfer at the air/water interface. Therefore, we focused our attention during this study on the measurements of mass accommodation coefficients of different hydrogen halides, i.e., HCl, HBr, and HI, which are presumably produced during halogen activation episodes. Note that the data derived here have a larger spectrum of applications since, for example, HCl is present in all the troposphere due to volcanoes emissions and/or emissions from a variety of industrial sources ranging from incinerators to perchlorate-fueled space vehicles!

## Experimental Section

The rate of uptake of a trace gas by a liquid is a multistep process that can be related to fundamental properties of the gas, of the interface, and of the condensed phase such as mass accommodation coefficient ($\alpha$), solubility, and reactivity. The rate at which a trace gas molecule may be transferred into the condensed phase can be obtained from the kinetic theory of gases. This allows the calculation of the net flux $\Phi_{net}$ that may cross the interface,

* Corresponding author. E-mail: george@illite.u-strasbg.fr.

† Current address: Laboratoire d'Application de la Chimie à l'Environnement (LACE), Bat. 303, 43 Bd du 11 Novembre 1918, F-69622 Villeurbanne Cedex, France.

10.1021/jp992621o CCC: $19.00 
Published on Web 12/11/1999

$$\Phi_{net} = \frac{1}{4}\langle c\rangle n\gamma \quad (1)$$

where $\langle c\rangle$ is the trace gas average thermal velocity, $\gamma$ is the uptake coefficient (taking into account all processes potentially affecting the uptake rate and therefore including $\alpha$), and $n$ is the gas-phase density of the trace gas.

The technique used to measure the uptake rates has already been described elsewhere,[14,15] and therefore, we will only provide a brief summary of its principle of operation. The uptake coefficient is measured by the decrease of the gas-phase concentration of the trace species, due to their exposure to a monodispersed train of droplets. These latter are generated by a vibrating orifice (75 $\mu$m diameter) leading to droplet diameters in the range 80−150 $\mu$m.

The apparatus, where the contact between both phases takes place, is a vertically aligned flowtube which internal diameter is 1.8 cm. Its length can be varied up to 20 cm, to change the gas/liquid interaction time (0−20 ms) or the surface exposed by the droplet train (0−0.2 cm$^2$). Since the uptake process is directly related to the total surface $S$ exposed by the droplets, any change $\Delta S$ in this surface results in a change $\Delta n$ of the trace gas density at the exit ports of the flowtube. Considering the kinetic theory of gases and since we are measuring the averaged signal during the transit time due to changes in the exposed surface, it becomes possible to calculate the uptake rate as[16]

$$\gamma = \frac{4F_g}{<c>\Delta S}\ln\left(\frac{n}{n-\Delta n}\right) \quad (2)$$

where $F_g$ is the carrier gas volume flow rate through the system, $n$ is the trace gas density at the inlet of the flowtube and $\Delta n = n - n'$ where $n'$ is the trace gas density at the outlet port of the interaction chamber. By measuring the fractional changes in concentration $[n/(n - \Delta n)]$ as a function of $\langle c\rangle\ \Delta S/4F_g$, it becomes possible to determine the overall uptake coefficient $\gamma$ as shown in Figure 1.

Aqueous solutions used to prepare the droplets were made from Milli-Q water (18 MΩ cm) and reagent grade salts when necessary. The different gaseous hydrogen halides were obtained simply by bubbling a known flux of He in an aqueous solution of the corresponding acid. If the latter was not enough concentrated, the solution was acidified with sulfuric acid in order to enhance the amount of hydrogen halide swept out of the solution by the helium flux. The resulting HX concentrations in the helium flux were in the range $10^{12}-10^{14}$ cm$^{-3}$ with most experiments performed with a density of about $10^{13}$ cm$^{-3}$. The gas-phase concentration was monitored using an ion-trap mass spectrometer (Varian model Saturn 4D) connected to the exit ports of the flowtube. For that purpose, a small flux of helium (ca. 1 cm$^3$ STP) was continuously sampled through a 50 $\mu$m pinhole, diluted with pure helium and then directly injected into the high vacuum chamber of the ion trap through a ca. 15 cm long heated glass tube (i.d., 1 cm). The gases were then ionized with an electron beam with an energy of 70 eV. A full mass spectrum was taken every second.

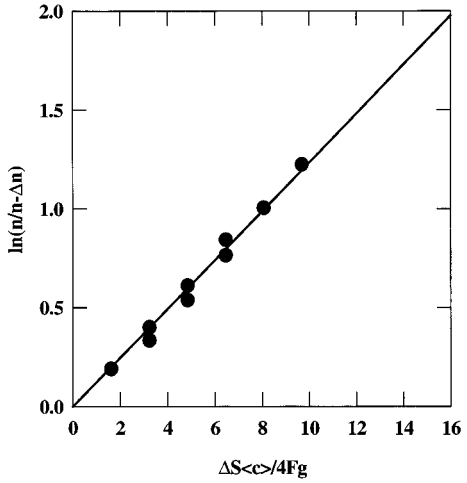


**Figure 1.** Typical plots of $\ln(n/n - \Delta n)$ versus $\langle c\rangle\Delta S/4F_g$ for $N_2O_5$ on pure water at 267 K for HCl. According to eq 2, the slopes of such plots are a measure of the uptake coefficient $\gamma$. The solid line represents a linear fit to our data.

**TABLE 1: Henry's Law Constant and Dissociation Constants for HCl, HBr, and HI at 298 K[11,39−41]**

| | physical Henry's law constant[a] (M atm$^{-1}$) | dissociation constant[b] (M) | chemical Henry's law constant[c] (M atm$^{-1}$) |
|---|---|---|---|
| HCl | 1 | $10^7$ | $1.3 \times 10^9$ |
| HBr | 0.75 | $10^9$ | $2.0 \times 10^6$ |
| HI | 2.5 | $3.2 \times 10^9$ | $2.5 \times 10^9$ |

[a] From refs 11, 40, and 41. [b] From ref 39. [c] From refs 40 and 41.

All gases used during this study are highly sticky. Therefore, to achieve a rapid steady state of the adsorption−desorption processes at the flowtube wall's, all the gas delivery system (including the flowtube itself) was heated to 310−320 K. With such experimental conditions, any change of the gas-phase density as monitored by mass spectrometry was simply related to the uptake by the droplets as shown by the first order kinetics which was measured (see Figure 1). It must also be underlined that due to the moveable outlet of the flowtube, its inner glass surface-to-volume ratio was systematically varied by a factor of 2. With such a variation, any wall effects would have been easily detected, which was not the case during this study.

## Results

All acids studied here have large effective Henry's law constants due to their dissociation according to

$$HX + H_2O \Leftrightarrow X^- + H_3O^+ \quad (3)$$

where X is either Cl, Br, or I. Table 1 lists the effective Henry's law constant found in the literature. It should be mentioned that despite the large solubility of these acids, physical Henry's law (i.e., just referring to gas/liquid partitioning without dissociation) constants may be quite small. In fact, for HCl, the physical Henry's law constant was estimated to be on the order of 1 M atm$^{-1}$, whereas the chemical dissociation increases this value by several orders of magnitude.[17,18] It was found experimentally that the uptake rates of these acids were not dependent on the interaction time, meaning that saturation effects were absent. In such a case, the uptake coefficient may be described according to[16]

$$\frac{1}{\gamma} = \frac{\langle c\rangle d_{eff}}{8D_g} - \frac{1}{2} + \frac{1}{\alpha} \quad (4)$$

where $d_{eff}$ is the effective droplet diameter.[16] The diffusion coefficient ($D_g$) is not known and therefore had to be estimated by the method presented by Reid et al.[19] In addition, since our carrier gas is a mixture of helium and water vapor, it was necessary to compute the diffusion coefficient in this background. This was done according to the following equation:

$$\frac{1}{D_g} = \frac{P_{H_2O}}{D_{g-H_2O}} + \frac{P_{He}}{D_{g-He}} \quad (5)$$

where $P_{H_2O}$ and $P_{He}$ are the partial pressures of water and helium respectively, $D_{g-H_2O}$ and $D_{g-He}$ are the binary diffusion coefficients of the trace gases in water and helium respectively (see Table 2 for numerical values).

Uptake rate measurements were performed on pure water but also on 1 M NaOH solutions. It was found that the uptake kinetics were strictly identical on pure water or on NaOH solutions, i.e., independent of the interaction time. This means that the measured uptake rates were not affected by any saturation effects which could have been introduced by a too strong acidification of the surface, due to the in-coming acid nor to a low dissociation process. In fact, it can be safely assumed that reaction 3 is faster in alkaline solutions meaning that if the uptake is limited by the dissociation kinetics, these effects should vanish at pH 14 used in some of our experiments. Therefore, the observed uptake rates should have been larger on solutions with pH = 14 than on pure water. Since this was not the case, we assume that we are measuring only the forward rate of the entry of the trace gas into a liquid and that eq 4 fully applies to our system.

Figure 2 shows the mass accommodation coefficients obtained, as a function of temperature, once the uptake coefficients have been corrected for diffusion limitations using eq 4. The ratio between the measured uptake coefficients and the calculated mass accommodation coefficients were in the range 1.3−1.7, highlighting the strong interplay between diffusion and interfacial transports. Also, by lowering the temperature, the mixed diffusion coefficient was affected, but we believe that this introduces only a slight error since the temperature range of our measurements is restricted (because both of the properties of water and of our experimental setup), meaning that the influence of the changes of water partial pressure is also limited. However, in all cases, it was estimated that the diffusion coefficients and partial pressures of the gases were known to within 30%. Such an uncertainty will in turn introduce an additional error on α of about the same level. Please note that the errors given below are just reflecting the experimental uncertainties and are given at the $2\sigma$ level.

The α values exhibit a clear negative dependence with temperature. For example, in the case of HBr, α decreases from

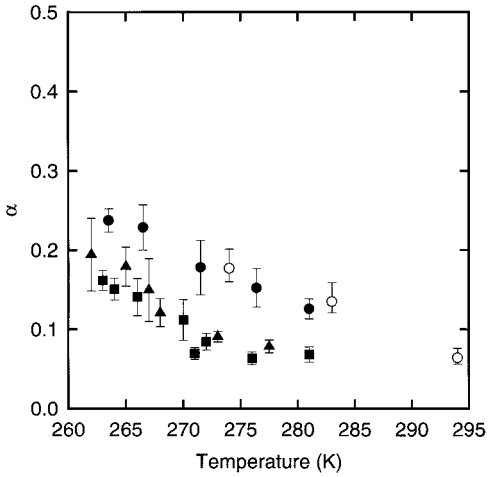


**Figure 2.** Plot of α versus temperature for HCl, HBr, and HI. The error bars are given at the $2\sigma$ level. (circles, HCl; squares, HBr; triangles, HI; filled symbols, this work; hollow circles, HCl from ref 17).

**TABLE 2: Gas-Phase Diffusion Coefficients, at 298 K and 1 atm, Estimated for the Hydrogen Halides using Methods Described by Reid et al.[19]**

| | $D_{g-H_2O}$ | $D_{g-He}$ |
|---|---|---|
| HCl | 0.23 | 0.62 |
| HBr | 0.20 | 0.60 |
| HI | 0.18 | 0.52 |

0.16 to 0.068 when the temperature increases from 262 to 281 K. It is also apparent that the mass accommodation coefficients exhibit the following trend: $\alpha_{HCl} > \alpha_{HBr} \approx \alpha_{HI}$. Figure 2 also shows the excellent agreement with the previously published results obtained by Van Doren et al.[17] on HCl, leading to an increased level of confidence in the reported mass accommodation coefficients in both studies. The agreement with other studies[20−22] is also satisfactory despite different experimental conditions. In fact, Abul-Haj et al.[20] reported 0.1 as an upper limit for the mass accommodation coefficient of HCl on water, whereas Kirchner et al.[22] measured a lower limit for α of 0.01 at room temperature, i.e., our measured value lies between these two limits. These restricted sets of experiments were performed on water, but many more data were published for the uptake of HCl on ice or sulfuric acid.[23−33] Although the nature of the surfaces are different, some similarities can be noted in the uptake rates, especially when high concentrations of HCl in the gas phase ($>10^{12}$ molecules/cm$^3$) have been used.

When studying the HCl uptake on ice, it was observed that the initial uptake is very fast but decreased to a value $<0.01$[29] after a few minutes. However, when high HCl concentrations were used, there was unlimited uptake and no sign of saturation was noted, a situation very similar to the one observed in the present study. A possible explanation is that a supercooled layer of liquid forms on the surface of the ice, and large uptake can be sustained due to the rapid diffusion of HCl in the liquid phase (as compared to solid). Under such conditions, the agreed lower limit for α is 0.3 for a temperature range 191−211 K. Of course, for these temperatures, our extrapolated value would be larger than 0.3, but it must be remembered that 0.3 represents a lower value. Our value would be in agreement with recent simulations yielding a theoretical accommodation coefficient of unity.[34]

The observed negative temperature dependence of α seems to be a general feature for the mass accommodation process of soluble nonreacting gases (see refs 35−37 for a complete discussion). In this case and in order to describe the temperature dependence, several authors have considered that mass accommodation can be viewed as a multistep process where the trace gas first thermally accommodates on the droplet surface (with the assumption that the adsorption coefficient is close to unity) and remains adsorbed until it undergoes a further step into the liquid or until it is released back to the gas phase. Davidovits et al.[35] hypothesised that the rate-limiting step in the mass accommodation is part of the physical solvation process. Therefore, the transition from the gas phase into the liquid phase can be summarized as[37]

$$n_g \underset{k_{desorb}}{\overset{k_{ads}}{\rightleftharpoons}} n_s \xrightarrow{k_s} n_s^* \xrightarrow{k_{sol}} n_l \quad (6)$$

where the subscripts g, s, and l refer to the gas, surface, and liquid state of the trace gas. Since the interface is a dynamic region where water clusters are formed and destroyed continuously, the solvation process is expected to involve the formation of liquidlike clusters. As in classical theory of nucleation, only clusters reaching a critical size ($n_s^*$ in eq 6) may grow indefinitely and finally merge with the nearby liquid. The critical

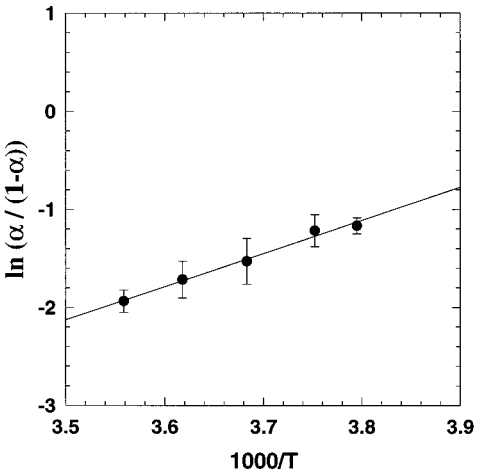


**Figure 3.** Representation of $\ln(\alpha/1-\alpha)$ versus $1/T$ according to eq 8 for HCl. The solid line represents a linear fit to our data and its results given value of $\Delta H^{\neq}_{obs}$ and $\Delta S^{\neq}_{obs}$. The error bars are given at the $2\sigma$ level.

size $N^*$ is defined as the number of molecules in the cluster or more precisely the number of hydrogen bonds used to form the cluster. The mass accommodation coefficients therefore reflect the competition between the rate of solvation ($k_{sol}$) and especially of cluster formation ($k_s$ which is proportional to $k_{sol}$) and desorption ($k_{desorb}$) of the surface species. By considering this model, the flux of molecules crossing the interface (eq 1) can be rewritten as

$$\frac{1}{4}\langle c\rangle n_g\alpha = \frac{1}{4}\langle c\rangle n_g - n_s k_{desorb} = n_s k_{sol} \qquad (7)$$

By considering that both $k_{sol}$ and $k_{desorb}$ can be expressed by an Arrhenius exponential temperature dependence relationship, eq 7 can be rearranged, leading to

$$\ln\left\{\frac{\alpha}{1-\alpha}\right\} = -\frac{\Delta G^{\neq}_{obs}}{RT} \qquad (8)$$

where $\Delta G^{\neq}_{obs}$ can be regarded as the height of the Gibbs free energy barrier between the gas and the surface transition state. The enthalpy $\Delta H_{obs}$ and entropy $\Delta S_{obs}$ can be derived from a plot of $\ln(\alpha/1-\alpha)$ versus $1/T$ as displayed in Figure 3 for HCl. The slope of such a plot corresponds to $-\Delta H_{obs}/R$, while the intercept corresponds to $\Delta S_{obs}/R$. The values obtained for $\Delta S_{obs}$ and $\Delta H_{obs}$ are summarized in Table 3.

By applying this treatment to our data, we implicitly assumed that the rate-limiting step for the uptake of the hydrogen halides is part of the physical solvation process and that the chemical solvation (or acid−base dissociation) can be decoupled from that process, i.e., it takes place after the physical step. Of course, the experiments here are made at a macroscopic scale and will give only poor insight into the molecular processes occurring at the interface. Nevertheless, the similarity of behavior of these reactive hydrogen halides with the one observed for nonreactive gases is supporting the observation that the common rate-limiting step is introduced by a physical process. In this context,

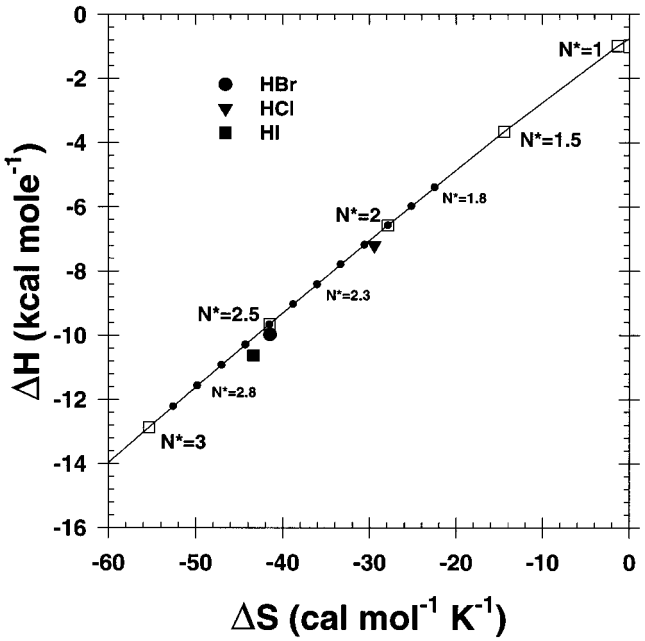


**Figure 4.** Relationship between $\Delta S$ and $\Delta H$ as given by Nathanson et al.[37] Filled symbols are the critical cluster size measured for the hydrogen halides.

it seems clear that one of the clues could be found in the Gibbs free energy $\Delta G^{\neq}_{obs}$ which is certainly related to fundamental properties of the incoming gas and, as underlined in previous work, especially to its ability to form hydrogen bonds with water which are thought to be the driving force for the formation of clusters. Davidovits et al.[35] and Nathanson et al.[37] demonstrated a direct relationship between $\Delta H_{obs}$, $\Delta S_{obs}$, and the size of the critical cluster governed by $N^*$. Therefore, this latter parameter can be determined from the values of the enthalpy and entropy given in Table 3. A graphical representation of this relationship is given in Figure 4, whereas numerical values are listed in Table 3.

As it can be seen from Table 3, the critical size increases from 2.1 to 2.6 when going from HCl to HI (noninteger values may be regarded as average sizes). This trend seems to inversely follow the capacity of hydrogen bonding of the hydrogen halides. In fact, by looking at fundamental properties of these acids (as listed in Table 3) such as dipole moment, partial charge, ... and, as finally expected, the charge of both halogen and hydrogen is decreasing when going from HCl to HI. This behavior would support the fact that mass accommodation proceeds via H-bonding, first at the interface and later in the bulk of the droplets. However, with regard to the limited data set reported here (i.e., only three hydrogen halides were studied), it seems difficult to find a relation that may correlate for example the dipole moment of a given chemical bonding to its contribution to the critical cluster size.

## Atmospheric Implications

By considering the theoretical work of Schwartz,[38] it possible to calculate the upper limit for the uptake rate due to gas-phase

**TABLE 3: Estimated Critical Cluster Size $N^*$ and Fundamental Properties of the Hydrogen Halides**

| | $N^*$ | dipole moment ($D$) | HX bond length (Å) | partial charge | electronegativity of X (Pauling) | $\Delta S_{obs}$ (cal mol$^{-1}$ K$^{-1}$) | $\Delta H_{obs}$ (kcal mol$^{-1}$) |
|---|---|---|---|---|---|---|---|
| HCl | 2.10 | 1.11 | 1.27 | 0.18 | 3.16 | $-29.4 \pm 4.6$ | $-7.2 \pm 1.0$ |
| HBr | 2.50 | 0.83 | 1.41 | 0.12 | 2.96 | $-41.5 \pm 7.5$ | $-10.0 \pm 1.8$ |
| HI | 2.60 | 0.45 | 1.61 | 0.06 | 2.66 | $43.4 \pm 4.6$ | $-10.6 \pm 1.1$ |

diffusion ($R_g^{max}$) and interfacial mass transport ($R_{int}^{max}$) according to

$$R_g^{max} = \frac{6D_g P_{HX}}{RTd^2} \quad (9)$$

$$R_{int}^{max} = \frac{6P_{HX}\langle c\rangle\alpha}{4RTd} \quad (10)$$

where $P_{HX}$ is the partial pressure of the hydrogen halides of interest (assumed to be equivalent to 2 ppt for all of them in the present calculations) and $d$ is the diameter of the droplet considered. At 273 K, where all mass accommodation coefficients are larger than 0.1, it appears from these simple equations that gas-phase diffusion is the limiting step during the uptake on droplets having diameter larger than 4 $\mu$m, otherwise the interfacial mass transport will influence the overall kinetics. The latter situation will be observed for film drops and secondary aerosols within the boundary layer, meaning that the accommodation process has to be carefully addressed in models devoted to a simulation within this part of the atmosphere.

In conclusion, the reported data support the fact that the mass accommodation process proceeds primarily through hydrogen bonding at the air/water interface. The reported temperature dependences were used in order to extract from the kinetic data information free energy changes during the uptake that allowed estimation of the critical size of the cluster formed during the accommodation as described in the currently accepted model.

**Acknowledgment.** Support for this work by the European Commission under Contract ENV4-CT97-0388, Project "Model Development for Atmospheric Aqueous Phase Chemistry (MODAC)" and by the CNRS (Program National de Chimie Atmosphérique, PNCA) is gratefully acknowledged.

## References and Notes

(1) Kolb, C. E.; Worsnop, D. R.; Zahniser, M. S.; Davidovits, P.; Hanson, D. R.; Ravishankara, A. R.; Keyser, L. F.; Leu, M. T.; Williams, L. R.; Molina, M. J.; Tolbert, M. A. In *Advances in Physical Chemistry Series*; Barker, J. R., Ed.; World Scientific: Singapore, 1994 Vol. 3.

(2) Barrie, L. A.; Bottenheim, J. W.; Schnell, R. C.; Crutzen, P. J.; Rasmussen, R. A. *Nature* **1988**, *334*, 138.

(3) Behnke, W.; George, C.; Scheer, V.; Zetzsch, C. *J. Geophys. Res.* **1997**, *102*, 3795.

(4) Martens, C. S.; Wesolowski, J. J.; Harriss, R. C.; Kaifer, R. *J. Geophys. Res.* **1973**, *78*, 8778.

(5) Keene, W. C.; Pzenny, A. P.; Jacob, D. J.; Duce, R. A.; Galloway, J. N.; Schultz-Tokos, J. F.; SieveringBoatman *Global Biogeochem Cycles* **1990**, *4*, 407.

(6) Frenzel, A.; Scheer, V.; Sikorski, R.; George, C.; Behnke, W.; Zetzsch, C. *J. Phys. Chem. A* **1998**, *102*, 1329.

(7) Schweitzer, F.; Mirabel, P.; George, C. *J. Phys. Chem. A* **1998**, *102*, 3942.

(8) Fickert, S.; Helleis, J.; Adams, J.; Moortgart, G. K.; Crowley, J. N. *J. Phys. Chem. A* **1998**, *102*, 10689.

(9) Caloz, F.; Seisel, S.; Fenter, F. F.; Rossi, M. J. *J. Phys. Chem. A* **1998**, *102*, 7470.

(10) Vogt, R.; Crutzen, P. J.; Sander, R. *Nature* **1996**, *383*, 327.

(11) Sander, R.; Crutzen, P. J. *J. Geophys. Res.* **1996**, *101*, 9121.

(12) Platt, U.; Janssen, C. *Faraday Discussion* **1995**, *100*.

(13) Wingetener, O. W.; Kubo, M. K.; Blake, N. J.; Smith, T. W., Jr.; Blake, D. R.; Rowland, F. S. *J. Geophys. Res.* **1996**, *101*, 4331.

(14) Schweitzer, F.; Magi, L.; Mirabel, P.; George, C. *J. Phys. Chem. A* **1998**, *102*, 593.

(15) Magi, L.; Schweitzer, F.; Pallares, C.; Cherif, S.; Mirabel, P.; George, C. *J. Phys. Chem. A* **1997**, *101*, 4943.

(16) Worsnop, D. R.; Zahniser, M. S.; Kolb, C. E.; Gardner, J. A.; Jayne, J. T.; Watson, L. R.; Van Doren, J. M.; Davidovits, P. *J. Phys. Chem.* **1989**, *93*, 1159.

(17) VanDoren, J. M.; Watson, L. R.; Davidovits, P.; Worsnop, D. R.; Zahniser, M. S.; Kolb, C. E. *J. Phys. Chem.* **1990**, *94*, 3265.

(18) Clegg, S. L.; Brimblecombe, P. *Atmos. Environ.* **1986**, *20*, 2483.

(19) Reid, R. C.; Prausnitz, J. M.; Poling, B. E. *The properties of gases and liquids*, 4th ed.; McGraw-Hill: New York, 1987.

(20) Abul-haj, N. A.; Martin, L. R.; Brenner, D. M. *AIP Conf. Proc. (Adv. Laser Sci. 3)* **1987**, *172*, 773.

(21) Adewuyi, Y. G.; Carmichael, G. R. *Atmos. Environ.* **1982**, *16*, 719.

(22) Kirchner, W.; Welter, F.; Bongartz, A.; Kames, J.; Schweighoefer, S.; Schurath, U. *J. Atmos. Chem.* **1990**, *10*, 427.

(23) Abbatt, J. P. D.; Molina, M. J. *Geophys. Res. Lett.* **1992**, *19*, 461.

(24) Abbatt, J. P. D.; Molina, M. J. *J. Phys. Chem.* **1992**, *96*, 7674.

(25) Abbatt, J. P. D.; Beyer, K. D.; Fucaloro, A. F.; Mcmahon, J. R.; Wooldridge, P. J.; Zhang, R.; Molina, M. J. *J. Geophys. Res.* **1992**, *97*, 15819.

(26) Chu, L. T.; Leu, M. T.; Keyser, L. F. *J. Phys. Chem.* **1993**, *97*, 7779.

(27) Elrod, M. J.; Koch, R. E.; Kim, J. E.; Molina, M. J. *Faraday Discuss.* **1995**, 269.

(28) Fluckiger, B.; Thielmann, A.; Gutzwiller, L.; Rossi, M. J. *Ber. Bunsen-Ges. Phys. Chem.* **1998**, *102*, 915.

(29) Hanson, D. R.; Ravishankara, A. R. *J. Phys. Chem.* **1992**, *96*, 2682.

(30) Hanson, D. R.; Ravishankara, A. R. *J. Phys. Chem.* **1993**, *97*, 12309.

(31) Henson, B. F.; Wilson, K. R.; Worsnop, D. R.; Casson, J. L.; Noble, C.; Robinson, J. M. *Abstracts of papers of the American Chemical Society* **1997**, *214*, 400.

(32) Hitchcock, D. R.; Spiller, L. L.; Wilson, W. E. *Atmos. Environ.* **1980**, *14*, 165.

(33) Luo, B. P.; Clegg, S. L.; Peter, T.; Muller, R.; Crutzen, P. J. *Geophys. Res. Lett.* **1994**, *21*, 49.

(34) Wang, L.; Clary, D. C. *J. Chem. Phys.* **1996**, *104*, 5663.

(35) Davidovits, P.; Jayne, J. T.; Duan, S. X.; Worsnop, D. R.; Zahniser, M. S.; Kolb, C. E. *J. Phys. Chem.* **1991**, *95*, 6337.

(36) Davidovits, P.; Hu, J. H.; Worsnop, D. R.; Zahniser, M. S.; Kolb, C. E. *Faraday Discuss.* **1995**, 65.

(37) Nathanson, G. M.; Davidovits, P.; Worsnop, D. R.; Kolb, C. E. *J. Phys. Chem.* **1996**, *100*, 13007.

(38) Schwartz, S. E. In *NATO ASI Series*; Jaeschke, W., Ed.; Springer-Verlag: Berlin Heidelberg, 1986; Vol. 4, p 415.

(39) Arnaud, P. *Cours de chimie organique*, 3rd ed.; Gauthier-Villars: Paris, 1966.

(40) Brimblecombe, P.; Clegg, S. L. *J. Atmos. Chem.* **1988**, *7*, 1.

(41) Marsh, A. R. W.; McElroy, W. J. *Atmos. Environ.* **1985**, *19*, 1075.